Facile and Efficient Route for Preparation of Polypyrrole-ZnO Nanocomposites: Microstructural, Optical, and Charge Transport Properties

M. A. Chougule,[1] S. Sen,[2] V. B. Patil[1]

[1]*Materials Research Laboratory, School of Physical Sciences, Solapur University, Solapur 413255, Maharashtra, India*
[2]*Crystal Technology Section, Technical Physics Division, BARC, Mumbai*

Received 9 July 2011; accepted 8 November 2011
DOI 10.1002/app.36475
Published online 1 February 2012 in Wiley Online Library (wileyonlinelibrary.com).

ABSTRACT: Polypyrrole (PPy) nanocomposites reinforced with zinc oxide (ZnONPs) nanoparticles are fabricated by spin coating method. The polymer nanocomposite films were characterized by X-ray diffraction (XRD), scanning electron microscopy (SEM), Fourier transform infrared (FTIR), UV-vis spectroscopy and two probe technique. The results were compared with PPy film. Powder XRD analysis demonstrates the crystalline structure of ZnO nanostructures, as well as their corresponding nanocomposites. The SEM images of the nanocomposites show uniform distribution of the ZnO NPs in the PPy matrix. The overall grain size was found to change in nanocomposite films. In the FTIR spectra, the characteristic peaks of pure PPy are observed to shift to higher wave number revels the different interfacial interactions between the ZnO NPs and the PPy matrix. In the UV-vis spectra, absorption peak of PPy shifts to lower wavelengths indicating poor conjugation. The electrical resistivity of PPy-ZnO nanocomposites is observed to depend strongly on the particle loadings and the morphology. © 2012 Wiley Periodicals, Inc. J Appl Polym Sci 125: E541–E547, 2012

Key words: PPy; ZnO; NPs; XRD; SEM; FTIR

INTRODUCTION

Recently, polymer nanocomposites have attracted great interest owing to their novel properties derived from the successful combination of the characteristics of parent constituents into a single material. The unparallel advantage such as cost-effective processability, lightweight and tunable mechanical, electrical and optical properties for the diverse applications such as microwave absorption layers, gas sensors, super capacitors.[1–4]

Conducting polymers such as polyaniline and polypyrrole (PPy) are becoming increasingly important for their technological importance due to their electrical, optical properties and their high air, chemical and electrical stability at ambient conditions.[5,6] PPy is a relatively air stable organic conducting polymer with high electrical conductivity, good environmental, chemical and electrical stability and easy synthesis.[7,8] The charge carriers of the PPy are generally considered to be polarons and bipolarons stabilized by counter ions incorporated into the polymer during preparation. Therefore, conducting and physical properties of PPy depend on the choice of counter ion called dopent.

Correspondence to: V. B. Patil (drvbpatil@gmail.com).
Contract grant sponsor: DAE-BRNS, 2010/37P/45/BRNS/1442.

Zinc oxide (ZnO), a versatile semiconductor material, has been attracting attention because of the commercial demand for optoelectronic devices operating at blue and ultraviolet regions.[9] ZnO is a wurtzite n-type semiconductor with band gap energy of 3.37 eV, and it has very large excitation binding energy (60 meV) at room temperature.[10] Recently, special attention has been devoted to the morphology, as ZnO can form different nanostructures.[11–13] Thermal stability, irradiation resistance, and flexibility to form different nanostructures are the advantages that expedite its potential wide applications in photodetectors,[14] surface acoustic wave devices,[15] ultraviolet nanolaser,[16] varistors,[17] solar cells,[18] gas sensors,[19] biosensors,[20] ceramics,[21] field emission,[22] and nanogenerator.[23]

In recent years, the development of inorganic/polymer hybrid materials on nanometer scale have been receiving significant attention due to a wide range of potential applications in optoelectronic devices[24–26] and in field effect transistors.[27] The inorganic fillers at nanoscale exhibit high surface to volume ratio and thus expected to modify drastically the electrical, optical, and dielectric properties of polymer. In general, the synthesis of hybrid of polymer/inorganic material has the goal of obtaining a new composite material having synergetic or complementary behaviors between the polymer and inorganic material.

In this article, we report the synthesis of PPy-ZnO nanocomposite films by spin coating technique and

TABLE I
Thin Film Properties of PPy-ZnO Nanocomposites

Sr. No.	Composition	Thickness (μm)	Average crystallite size (from SEM)	Base resistivity (Ω cm)
1	PPy	0.132	0.45 μm	1.05×10^6
2	ZnO	0.29	67 nm	2.68×10^7
3	PZ (10%)	0.102	0.74 μm	2.85×10^6
4	PZ (20%)	0.106	0.77 μm	4.34×10^6
5	PZ (30%)	0.078	0.80 μm	5.34×10^6
6	PZ (40%)	0.108	0.84 μm	6.34×10^6
7	PZ (50%)	0.098	0.87 μm	7.01×10^6

study of their microstructural, morphological, optical, and charge transport properties.

EXPERIMENTAL DETAILS

Synthesis of PPy

PPy was synthesized by chemical oxidative polymerization technique using monomer pyrrole (C_4H_5N). Analytical grade ammonium per-sulphate (APS, $(NH_4)_2S_2O_8$) was used as an oxidizing agent. The chemical polymerization was carried out in a beaker by mixing 0.1M aqueous solution of pyrrole and 0.1M of APS in 1 : 1 ratio by volume. The polymerization was carried out at room temperature for a period of 4 h. After termination of polymerization process, black precipitate obtained. The precipitate was filtered and washed several times successively by distilled water to remove any possible oligomers and dried in oven at 60°C for 6 h and grind in pestle mortar to get PPy.[28]

Synthesis of ZnO nanoparticles

Nanocrystalline ZnO NPs has been synthesized by a sol–gel process using zinc acetate dihydrate [$Zn(Ac)_2{\cdot}2H_2O$] as a source for Zn.[29] The 5.393 g of $Zn(Ac)_2{\cdot}2H_2O$ was added to 40ml of methanol and mixture was stirred vigorously at 60°C for 1 h to form gel. After gel formation, heating was stopped and the solution was stirred continuously until the formation of a white powder. The powder was separated by filtration, washed several times with methanol and dried by dryer for 20 min. The powder was annealed in zone furnace at 700°C for 1 h to get the nanocrystalline ZnO NPs.

Synthesis of PPy–ZnO nanocomposite

The pure PPy and ZnO NPs were mixed together for making nanocomposites. The nanocomposites were prepared with different PPy-ZnO nanoparticles weight ratios (0–50%). These nanocomposites were dissolved in m-cresol and stirring it for 11 h. Polymer nanocomposite thin films were prepared by spin coating technique on glass substrates (10 × 10 mm) and dried at room temperature. Figure 1 shows synthesis scheme of PPy-ZnO nanocomposites.

Characterization techniques

X-ray diffraction (XRD) studies were carried out using a Philips powder X-ray diffractometer (Model: PW1710). The XRD patterns were recorded in the 2θ range of 20–80° with step width 0.02° and step time 1.25 s using CuK_α radiation ($\lambda = 1.5406$ Å). The XRD patterns were analyzed by matching the observed peaks with the standard pattern provided by JCPDS file. Fourier transform infra red (FTIR) spectroscopy (Model: Perkin Elmer 100) of ZnO, PPy, and PPy: ZnO (10–50%) composites were studied in the frequency range of 400–4000 cm^{-1}. Morphological study of the films of PPy and PPy: ZnO composite were carried out using scanning electron microscopy (SEM Model: JEOL JSM 6360) operating at 20 kV. UV-vis spectra of the samples, which were dispersed in deionized water under ultrasonic action, were recorded on a Simandzu −100 UV-Vis spectrophotometer. The electrical dc resistivity measurements were made on thin films using two probe techniques. The thickness of the PPy film, ZnO film, and PPy-ZnO film was measured by using Dektak profilometer and is given in Table I.

RESULTS AND DISCUSSIONS

X-ray diffraction

XRD spectra of PPy, ZnO NPs and PPy-ZnO (10–50 wt %) nanocomposites films are given in Figure 2. The XRD pattern of ZnO nanoparticles film is indexed to wurtzite structure having cell parameters $a = 3.253$ Å and $c = 5.21$ Å. This agrees with reported values $a = 3.29$ Å and $c = 5.20$ Å.[30,31] The XRD pattern of pure PPy film shows a amorphous peak at $2\theta = 24°$,[32,33] which indicates low degree of molecular ordering, this agrees with the oxidized state of PPy observed in UV-visible spectra. For PPy-ZnO nanocomposites films, presence of less intense ZnO diffraction peaks indicates that the ZnO nanoparticles are fully covered with a PPy. Compared

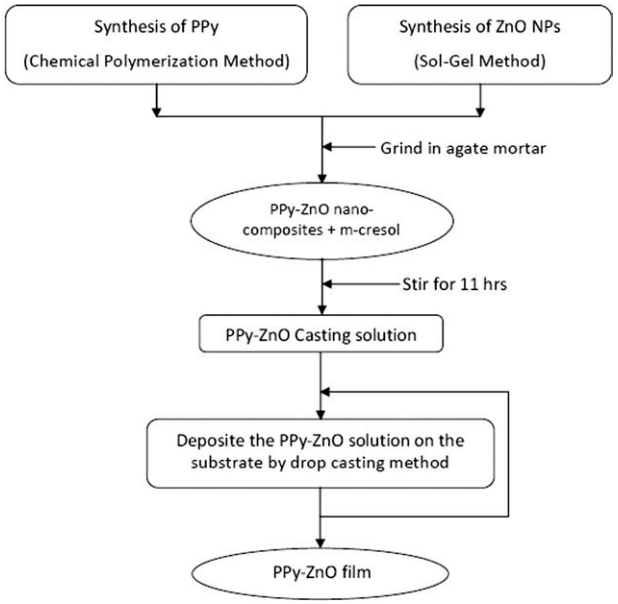

Figure 1 Flow diagram of synthesis and deposition of PPy-ZnO nanocomposite.

to the pure particles, the decrease in the intensities of the ZnO peaks in the polymer nanocomposites [Fig. 2(c)] suggests that the ZnO NPs are highly dispersed in the PPy matrix,[33] and the broadness of the peaks remains the same, which further suggests a uniform dispersion of the nanoparticles without serious agglomeration, as revealed by the SEM observation in Figure 3.

SEM

The morphologies of PPy, ZnO NPs, and PPy-ZnO (10–50%) nanocomposites are shown in Figure 3. Figure 3(a) shows the surface morphology of the PPy film. The microstructure of a PPy thin film has a uniform granular morphology and the average grain size is ~0.45 μm.[28] Figure 3(b) shows the surface morphology of the ZnO NPs film, annealed at 700°C for 1 h. The image shows that the ZnO NPs are fine with an average grain size of about 67 nm.[29] The SEM micrograph of composites of PPy and ZnO with different weight ratios are shown in Figure 3(c–g). Both pure PPy and its polymer nanocomposites are observed to exhibit particulate structures with a fairly uniform size distribution. The pure PPy particles are observed to be relatively loosely packed as compared with the polymer nanocomposites. For the polymer nanocomposites filled with different loadings of ZnO NPs, the particles are closely packed and no bare nanoparticles are observed even at the highest loading of 50 wt %, which suggests the feasibility of this method to fabricate well dispersed nanoparticles with uniform coating layer.

Fourier transform infra red analysis

Figure 4 shows the FTIR spectra of the pure PPy, ZnO NPs, and PPy-ZnO (10-50%) nanocomposites. For pure PPy, all the characteristics peaks are

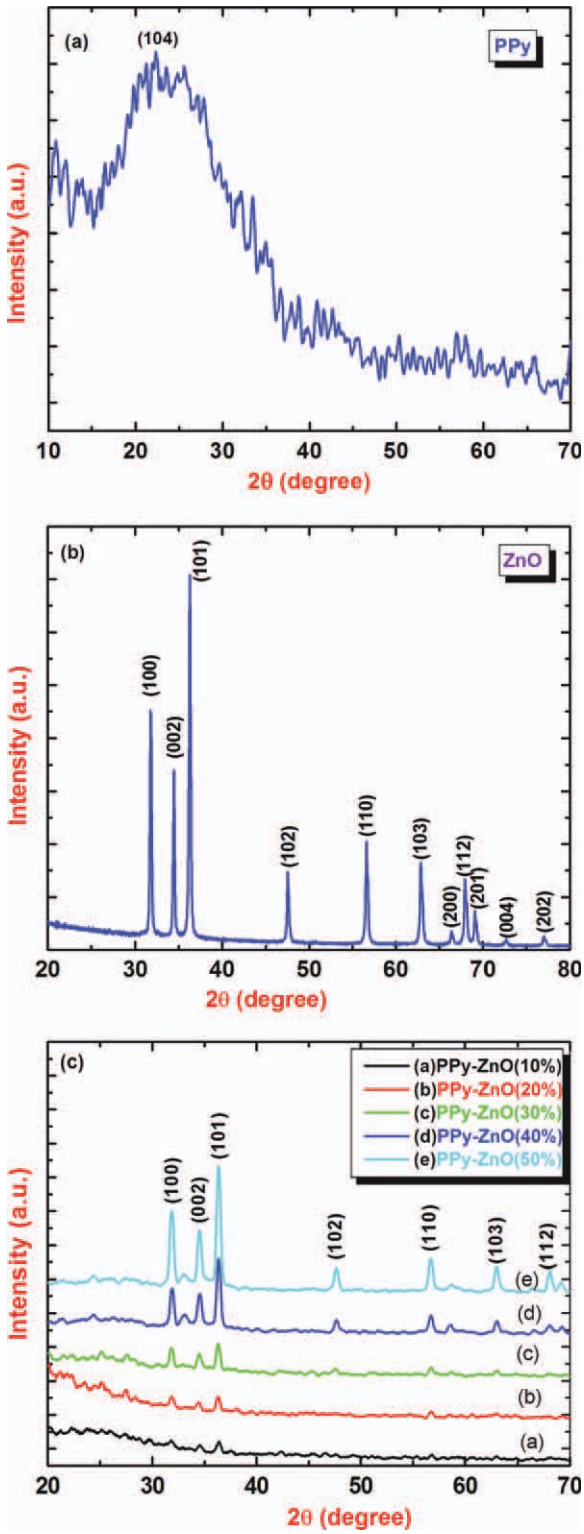

Figure 2 XRD pattern of (a) PPy, (b) ZnO, and (c-e) PPy-ZnO (10–50 %). [Color figure can be viewed in the online issue, which is available at wileyonlinelibrary.com.]

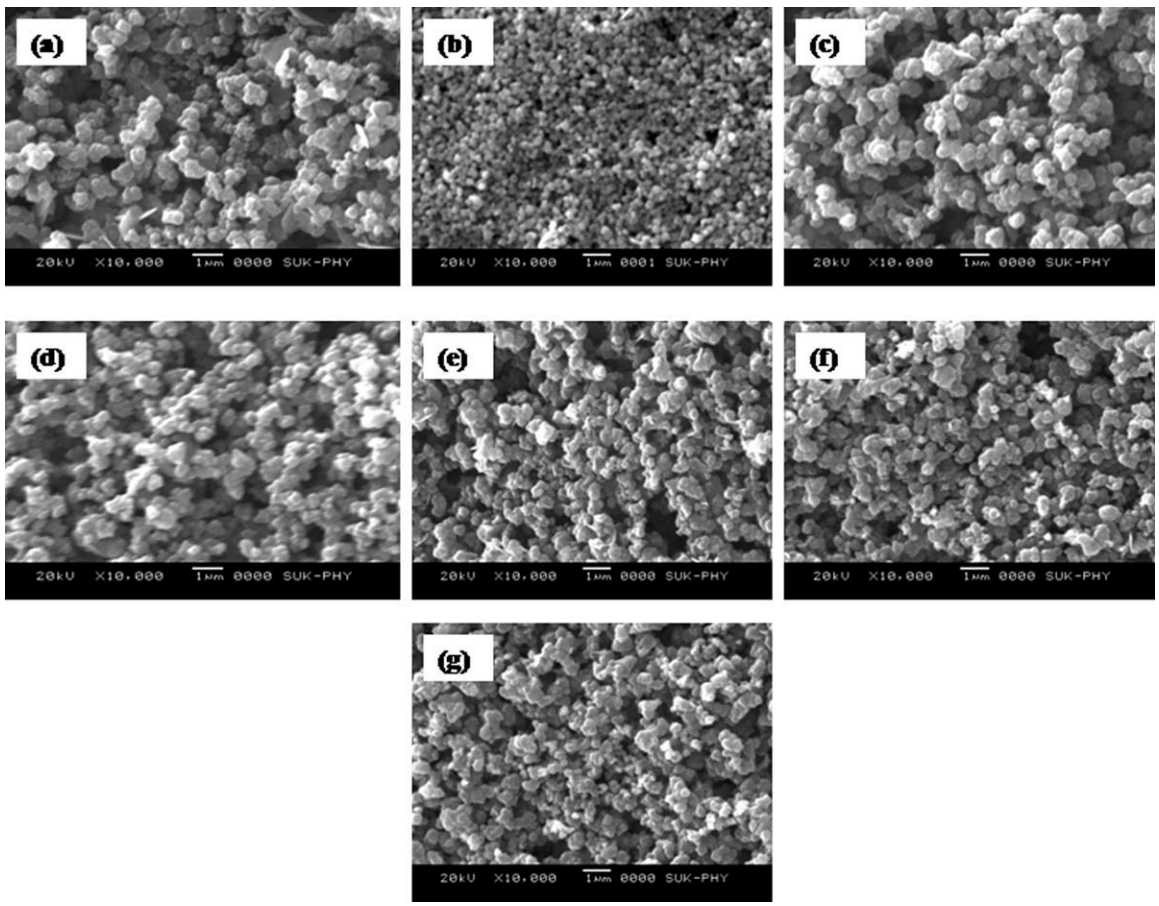

Figure 3 SEM images of (a) PPy, (b) ZnO, and (c-g) PPy-ZnO (10–50 %) nanocomposites.

observed at 794 cm^{-1} (=C—H wagging),[28,34,35] 926 cm^{-1} (C—C out of phase), 1048 cm^{-1} (=C—H in plane vibration), 1292 cm^{-1} (C—C bond), 1478 cm^{-1} (vibration of the pyrrole ring), 1558 cm^{-1} (C=C bond) and 1705 cm^{-1} (C=N bond). The small peak at 3115 cm^{-1} is assigned to presence of N-H stretching vibrations. The peaks observed in the present work match well with the ones available in literature,[35,36] confirming the formation of PPy. The spectrum for PPy-ZnO (10–50%) nanocomposites show some shift in the wavenumber as well as change in the intensity of peaks as compared to PPy. The most prominent changes are (i) shift of =C—H in plane vibration peak to low value from 1053 in PPy to 1045 cm^{-1}in composite film with increase in its intensity,(ii) shift of N—C structure bending to higher values from 1210 to 1203 $cm^{-1}$and (iii) peaks in PPy at 1478 and 1558 cm^{-1} corresponding to pyrrole ring vibration and C=C bond respectively got weakened in composite film. This change is due to loss in conjugation and molecular order after modification of PPy with ZnO. Since the frequency of a vibration is directly proportional to force constant of bonds, a shift in =C—H in-plane vibration to lower side indicate that the electrons are more localized in the pyrrole ring. This also indicates the shortening of N—C bonds, suggesting localization of π–orbital electrons on N. In addition, enhancement of the peak intensity of =C—H in-plane vibration indicates increase in the dipole moment .The results indicate interaction between PPy and ZnO nanoparticles. Thus after addition of ZnO nanoparticles there is strong localization of electrons over PPy ring and gets highly reduced from oxidized form.[35,36]

UV-VIS SPECTROSCOPY ANALYSIS

UV-Visible spectra were taken in order to study the effects of addition of ZnO nanoparticles in PPy structure. Spectra of PPy, ZnO NPs and PPy-ZnO (50%) nanocomposite films are shown in Figure 5. The band gap energy is calculated according to relation $\alpha = \alpha_0 (h\nu\text{-}E_g)^n$ ($n = 1/2$). Where α_0 is a constant α is the absorption coefficient, E_g is the optical band gap and $h\nu$ is the energy of incident photon. Band gap energy is calculated from spectra showing peaks of absorption at different wavelengths. PPy films and ZnO nanoparticles exhibits absorption peaks at 442 nm (2.81 eV) and 374 nm (3.33 eV), respectively, which are in good agreement with literature values.[37,38] In case of the PPy-ZnO(50%)

composite film, peaks due to PPy and ZnO nanoparticles shift to 429 nm (2.89 eV) and 378 nm (3.29 eV), respectively. As observed that the band gap of PPy

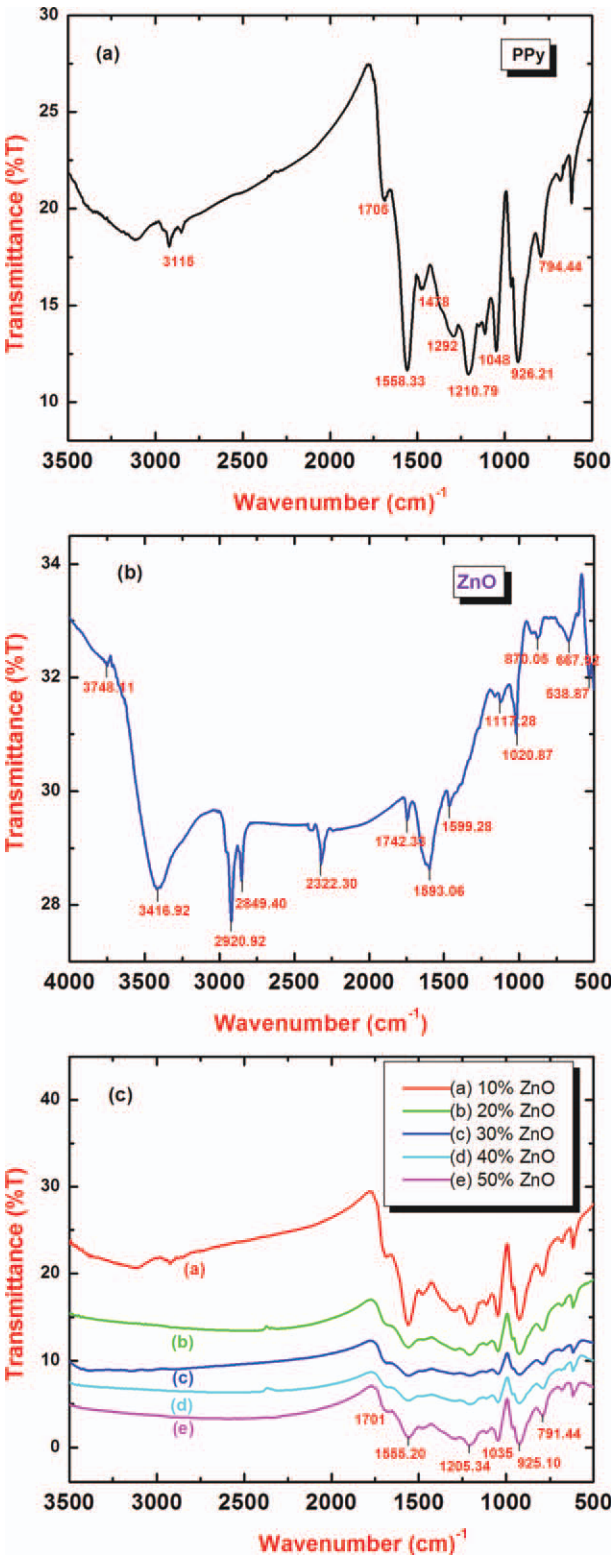

Figure 4 FT-IR spectra of (a) pure PPy, (b) ZnO NPs and (c) PPy-ZnO (10–50%). [Color figure can be viewed in the online issue, which is available at wileyonlinelibrary.com.]

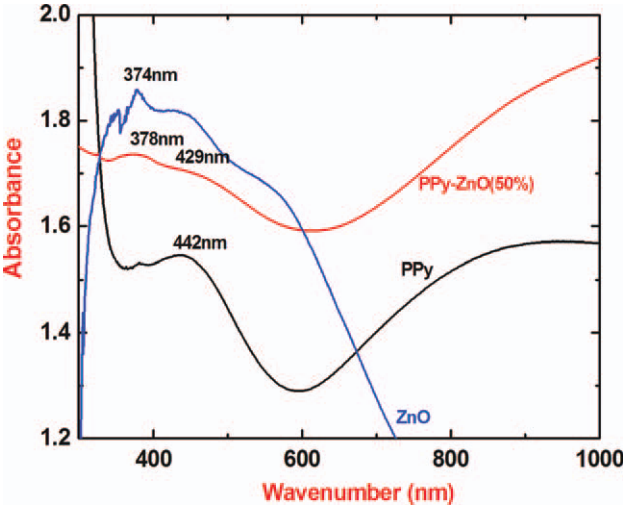

Figure 5 UV-visible spectra for PPy, ZnO and PPy-ZnO (50%) composite films. [Color figure can be viewed in the online issue, which is available at wileyonlinelibrary.com.]

increased whereas that for ZnO decreased indicating the interaction between PPy and ZnO nanoparticles. In the present work, there is a shift observed of absorption peak to lower wavelengths in case of PPy modified with ZnO nanoparticles indicative of poor conjugation. In the present results, for pure PPy film a broad peak at 2.81 eV is observed, which agrees with reported value,[39] indicating oxidized state of PPy. In PPy-ZnO (50%) nanocomposite film the peak shifts to higher energy that account to reduction of PPy after addition of ZnO NPs.[37,38]

ELECTRICAL RESISTIVITY STUDY

Figure 6 shows the variation of resistivity as a function of temperature for pure PPy, ZnO and PPy-ZnO (10–50 wt %) composites. Generally, the resistivity decreases with the increase of temperature, indicating the semiconducting behavior in the whole range of temperature.[40] It is found that the resistivity increases gradually with the particle loading increasing from 10 to 50% of ZnO NPs in the PPy matrix.

The typical values for resistivity of PPy and ZnO NPs film and variation of base resistivity with different proportions of PPy-ZnO nanocomposites are shown in Figure 7. The base resistivity of the composite film was found to be increasing with addition of ZnO nanoparticles content.

One of the interesting observations in Figure 6 is that the base resistivity of composite film is higher nearly one order in magnitude as compared to the pure PPy film. When n-type ZnO nanoparticle thin film is exposed to air, oxygen molecules adsorb on the surface of the ZnO nanoparticles and forms O_2^- ions by capturing electrons from the conduction

band. Thus ZnO nanoparticle films show a high resistance state in air.[41] The variation in the resistivity of the films from PPy through PPy-ZnO nanocomposite to ZnO is explained on the basis of granular morphology and in turn on intergrain and intragrain contribution to the resistivity.

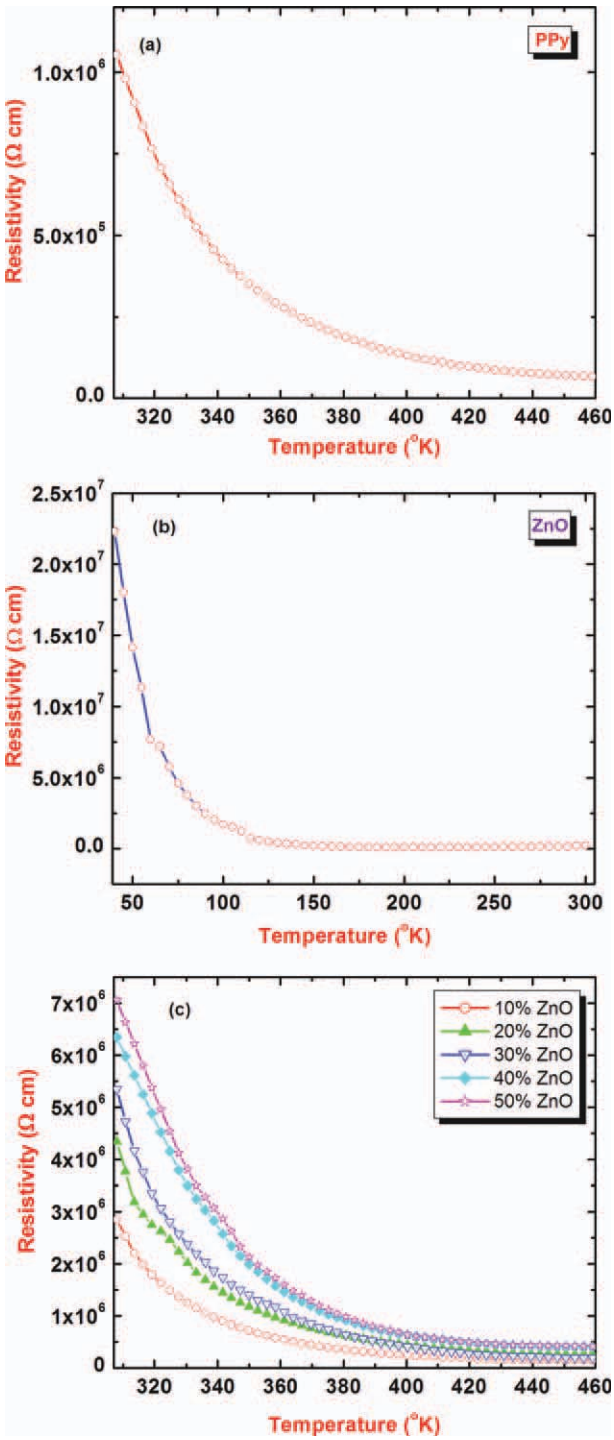

Figure 6 Plot of resistivity Vs temperature of (a) PPy (b) ZnO and (c) PPy-ZnO (10–50%). [Color figure can be viewed in the online issue, which is available at wileyonlinelibrary.com.]

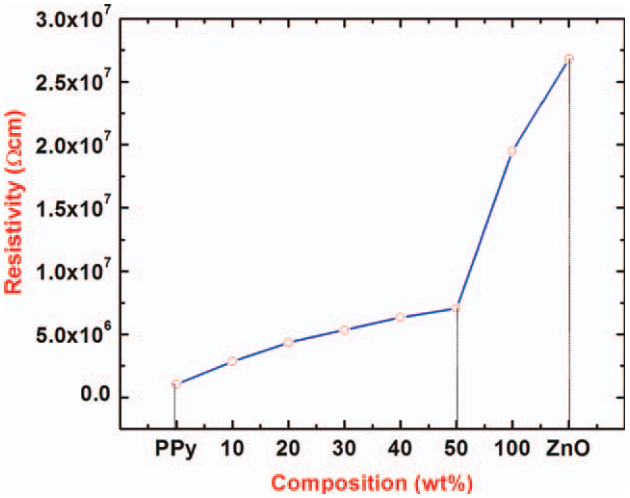

Figure 7 Plot of resistivity Vs ZnO content of nanocomposite films. [Color figure can be viewed in the online issue, which is available at wileyonlinelibrary.com.]

The granular morphology of the polymer film [Fig. 3(a)] indicates that the total resistivity (ρ) of the film can be expressed as:[42]

$$\rho = \rho_{intra} + \rho_{inter} + \rho_{ionic}.$$

ρ_{intra} is the contribution from the intragrain region and depends on the conjugation lengths(l) over which charge carriers are localized. In the case of non oriented polymer, ρ_{intra} varies as $1/\ln$ ($n = 3.2-3.5$), indicating that shorter the conjugation length higher is the resistivity.[42] If l is too short, then the charge transport is limited by interchain hopping. In fact, It can be altered by improving crystallinity and change in doping levels of conducting polymer. ρ_{inter} is the intergrain resistivity and depends on the height of the potential barrier formed at the grain boundaries. In general, smaller the grain size, higher is the value of ρ_{inter}. ρ_{ionic} is controlled by mobility of the counter of ions refs. [43–47]

In the present studies, as shown by SEM images (Fig. 3), ZnO nanoparticles get coated with polymer and are randomly distributed in the composite film. The grain size of the polymer is significantly enlarged in composite as compared with PPy indicating that conduction in composite films is largely due to polymer. Despite of an enhanced grain growth, the resistivity of the composite films increases dramatically, indicating that contribution from intergrain region is negligible. Since the ρ_{ionic} contribution is usually small, therefore an increase in resistivity of composite films can be attributed solely due to increase in ρ_{intra}.

CONCLUSIONS

The nanocomposites of PPy-ZnO have been successively prepared by spin coating method on glass

substrates. From structural studies (XRD), it is revealed that the intensities of the ZnO NPs peaks in the PPy-ZnO nanocomposites decreases, which suggests that the ZnO NPs are highly dispersed in the PPy matrix. The morphological studies (SEM) show uniform distribution of the ZnO particles in the PPy matrix. This indicates that ZnO NPs interact with PPy. The overall grain size is found to change in the composite film. From FTIR spectra, it is revealed that the characteristic absorption peaks of PPy shifted by significant amount into PPy-ZnO nanocomposite, which indicate the different interfacial interactions between the ZnO NPs and the PPy matrix. The UV-vis spectra show that the band gap of PPy-ZnO nanocomposites increases with increasing ZnO NPs indicating the interaction between PPy and ZnO NPs. The dc electrical resistivity increases gradually with increasing ZnO NPs into PPy matrix indicating the semiconducting behavior in the whole range of temperature.

References

1. Colin, P. Application of Conducting Polymers; Edited by R.H.H. Neubert and H.-H. Ruttinger, Dekker, New York, 2003.
2. Chehimi, M. M.; Abdelijalil, E. Synth Met 2004, 145, 15.
3. McQuade, D. T.; Pullen, A. E.; Swager, T. M. Chem Rev 2000, 100, 2537.
4. Gerard, M.; Chaubey, A.; Malhotra, B. D. Biosens Bioelectron 2002, 17, 345.
5. Anuar, K.; Murali, S.; Fariz, A.; Mahmud Ekramul, H. N. M. Mater Sci 2004, 10, 255.
6. Kassim, A.; Basar, Z. B.; Mahmud, H. N. M. E. Chem Sci 2002, 114, 155.
7. Annur, K.; Murali, S.; Fariz, A.; Mahmud Ekramul, H. N. M. Mater Sci 2004, 10, 255.
8. Kassim, A.; Basar, Z. B.; Mahmud Ekramul, H. N. M. E. Synth Met 2002, 119, 155.
9. Look, D. C. Mater Sci Eng B 2001, 80, 383.
10. Lieber, C. M. Solid State Commun 1998, 66, 5309.
11. Zhang, Y.; Suenaga, K.; Collies, C.; Iijima, S. Science 1998, 281, 973.
12. Vayssieres, L.; Keis, K.; Hagfeldt, A.; Lindquist, S.-E. Chem Mater 2001, 13, 4395.
13. Pan, Z. W.; Dai, Z. R.; Wang, Z. L. Science 2001, 292, 1947.
14. Rodriguez, J. A.; Jirsak, T.; Dvorak, J.; Sambasivan, S.; Fischer, D. J. J Phys Chem B 2000, 104, 319.
15. Shin, W.-C.; Wu, M.-S. J Cryst Growth 1994, 137, 319.
16. Huang, H. M.; Mao, S.; Feick, H.; Yan, H.; Wu, Y.; Kind, H.; Weber, E.; Russo, R.; Yang, P. D. Science 2001, 292, 1897.
17. Hung, N. T.; Quang, N. D.; Bernik, S. J Mater Res 2001, 16, 2817.
18. Cooray, N. F.; Kushiya, K.; Fujimaki, A.; Okumura, D.; Sato, M.; Ooshita, M.; Yamase, O. Jpn J Appl Phys 1999, 38, 6213.
19. Paneva, R.; Gotchev, D.; Sens Actuat A: Phys 1999, 72, 79.
20. Topoglidis, E.; Cass, A.; E. G.; Oregan, B.; Durrant, J. R. J Electroanal Chem 2001, 517, 20.
21. Gao, L.; Li, Q.; Luan, W. L. J Am Ceram Soc 2000, 85, 1016.
22. Xu, C. X.; Sun, X. W. Appl Phys Lett 2003, 83, 3806.
23. Gao, P. X.; Ding, Y.; Mai, W.; Hughes, W. L.; Lao, C. S.; Wang, Z. L. Science 2005, 309, 1700.
24. Beek, B. W. J. E.; Slooff, L. H.; Wienk, M. N.; Kroon, J. M.; Janseen, R. A. J. Adv Funct Mater 2005, 15, 1703.
25. Sui, X. M.; Shao, C. L.; Liu, Y. C. Appl Phys Lett 2005, 87, 113.
26. Olson, D. C.; Piris, J.; Colins, R. T.; Shaheen, S. E.; Ginley, D. S. Thin Solid Films 2006, 496, 26.
27. Xu, Z. X.; Roy, V. A. L.; Stallinga, P.; Muccini, M.; Toffanin, S.; Xiang, H. F.; Che, C. M. Appl Phys Lett 2007, 90, 223509.
28. Chougule, M. A.; Pawar, S. G.; Raut, B. T.; Mulik, R. N.; Patil, V.B. Soft Nanosci Lett 2011, 1, 6.
29. Patil, V. B.; Pawar, S. G.; Patil, S. L.; Krupanidhi, S. B. J Mater-Sci Mate Elect 2010, 41, 355.
30. Wang, Z. L.; Kong, X. Y.; Ding, Y.; Gao, P.; Yang, W. L.; Zhang, R. Adv Funct Mater 2004, 14, 943.
31. Ouyang, J. Y.; Li, Y. F. Polymer 1997, 38, 3997.
32. Hakansson, E.; Lin, T.; Wang, H.; Kaynak, A. Synth Met 2006, 156, 1194.
33. Hong, R.; Huang, J.; He, H.; Fan, Z.; Shao, J. Appl Surf Sci 2005, 242, 346.
34. Tai, H.; Jiang, Y.; Xie, G.; Jingjinghao, J. H. Int J Environ Anal Chem 2007, 87, 539.
35. Shiigi, H.; Kishimoto, M.; Yakabe, H.; Deore, B.; Nagaoka, T. Anal Sci 2002, 18, 41.
36. Cheah, K.; Forsyth, M.; Truong, V. T. Synth Met 1998, 94, 215.
37. Wang, Z. L.; Kong, X. Y.; Ding, Y.; Gao, P.; Hughes, W. L.; Yang, R.; Zhang, Y. Adv Funct Mater 2004, 14, 943.
38. Shiigi, H.; Kishimoto, M.; Yakabe, H.; Deore, B.; Nagaoka, T. Anal Sci 2002, 18, 41.
39. Bredas, J. L.; Scott, J. C.; Yakushi, K.; Street, G. B. Phys Rev B 1984, 30, 1023.
40. Chakrabarti, S.; Banerjee, D.; Bhattacharyya, R. J Phys Chem B 2002, 106, 3061.
41. Pawar, S. G.; Patil, S. L.; Chougule, M. A.; Mane, A. T.; Jundale, D. M.; Patil, V. B. Int J Polym Mater 2010, 59, 1.
42. Wan, Q.; Li, Q. H.; Chen, Y. J.; Wang, T. H.; He, X. L.; Li, J. P.; Lin, C. L. Appl Phys Lett 2004, 84, 3654.
43. Lee, J. H.; Ko, K. H.; Park, B. O. J Cryst Growth 2005, 247, 119–125.
44. Baughhhman, R. H.; Shacklette, L. W. Phys Rev B 1989, 39, 5872.
45. Thakre, P. R.; Bisrat, Y.; Lagoudas, D. C. J Appl Polym Sci 2010, 116, 191.
46. Wang, J. Zhang, L. Appl Polym Sci 2009, 111, 1549.
47. Zhang, S. J.; Li, Y. F.; Wang, X. L. J Appl Polym Sci 2004, 91, 3981.